CALCULATED EFFECTS OF VARYING REYNOLDS NUMBER AND DYNAMIC PRESSURE ON FLEXIBLE WINGS AT TRANSONIC SPEEDS

Richard L. Campbell
NASA Langley Research Center
Hampton, Virginia

INTRODUCTION

The recent dedication of the National Transonic Facility (NTF) marked the beginning of a new era of research in transonic wind tunnels. Soon tests will be performed on models of complete aircraft configurations at full-scale Reynolds and Mach numbers. This capability will also provide an excellent opportunity to evaluate the transonic aerodynamic computer codes that utilize boundary layer theory to model viscous effects. While the cryogenic operating temperatures of the NTF are responsible for some of the increased Reynolds number range, it will be necessary to utilize high tunnel pressures to fully exploit the high Reynolds number capability of this facility (see ref. 1). Because of the range of dynamic pressures to which a model may be subjected (up to about 7000 psf), it is highly desirable to account for model aeroelastic deformation when making calculations using the transonic computer codes.

This report describes a computational method which has been developed that includes the effects of static aeroelastic wing deflections in steady transonic aerodynamic calculations. This method, known as the Transonic Aeroelastic Program System (TAPS), interacts a 3D transonic computer code with boundary layer and a linear finite element structural analysis code to calculate wing pressures and deflections. The nonlinear nature of the transonic flow makes it necessary to couple the aerodynamic and structures codes in an iterative manner.

TAPS has been arranged in a modular fashion so that different aerodynamic or structures programs may be used with a minimum of coding changes required. A complete description of the development of TAPS is given in reference 2; this paper will present results obtained using two different aerodynamic codes in TAPS and correlate those results with experimental data.

DESCRIPTION OF TRANSONIC AEROELASTIC PROGRAM SYSTEM (TAPS)

A flow chart illustrating the method of analysis used in TAPS is shown in figure 1. An aerodynamic model and a structural wing model are first developed for the test configuration. The structural wing model is then run through the structures code to obtain an influence coefficient matrix, which is saved for later use in calculating wing deflections. An initial, unconverged run is made with the aerodynamics code to obtain wing pressures; these pressures are then interpolated from the aerodynamic grid to the structural grid and converted to the input format of the structures code by the first translator module. The structures code then solves for the wing deflections using the influence coefficient matrix and nodal forces determined from the calculated wing pressures. These deflections are interpolated back to the aerodynamics grid and arranged as an input file to update the configuration shape in the next aerodynamic calculation. This aerodynamic/structural cycle is automated and may be continued until both the wing pressures and deflections have converged to the satisfaction of the user. The convergence criteria used in this study were negligible shock movement or change in pressure levels between successive iteration cycles based on comparison of pressure distribution plots and wing tip deflection changes of less than 2 percent.

TAPS has been arranged in a modular fashion so that it would be relatively easy to use different aerodynamic or structural codes. For this study, two aerodynamic codes were used: WIBCO, an extended small-disturbance wing/body code with a 2D strip boundary layer (ref. 3); and TAWFIVE, a full-potential wing/body code coupled with a 3D integral boundary layer (ref. 4). The SPAR structural analysis program (ref. 5) was used to make the wing deflection calculations for all cases.

Including the aeroelastic deflections did not appear to have any adverse effect on the convergence of the aerodynamic calculations; no underrelaxation of the deflections was required. The boundary layer effects seemed to be a more important factor affecting the rate of convergence. The calculation of wing deflections was also relatively inexpensive, being less than 10 percent of the cost of an aerodynamic/structural cycle (which includes 30-50 aerodynamic iterations) and less than the cost of the boundary layer calculations.

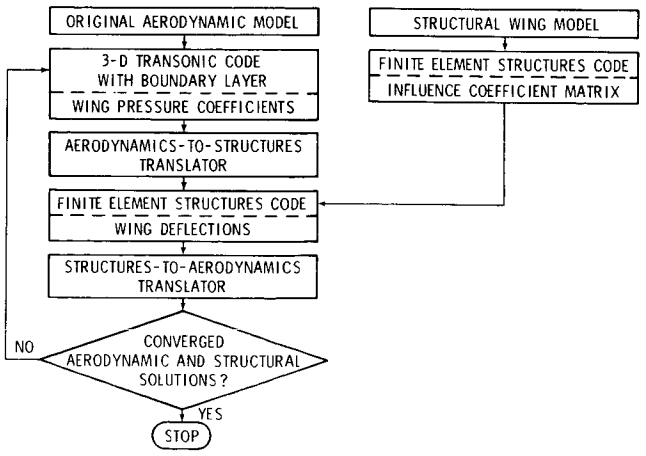

Figure 1

ADVANCED TECHNOLOGY TRANSPORT (ATT) MODEL DESCRIPTION

The first configuration used to evaluate TAPS was the Advanced Technology Transport (ATT) model (refs. 6 and 7). A top view of the right wing panel is shown in figure 2. The wing had a span of 45.0 in., a quarter-chord sweep of 33°, an aspect ratio of 7.498, and a taper ratio of 0.418. The airfoil sections were NASA supercritical designs with maximum thickness-to-chord ratios of 0.114 near the fuselage and 0.082 near the tip. A highly swept leading-edge glove extended from the fuselage to about $\eta = 0.35$ and there were four trailing-edge control surfaces (three inboard, one outboard). The wing was constructed of solid aluminum with channels for the pressure tubing machined into the upper and lower surfaces. Four main channels were cut into the wing approximately along lines of constant chord with smaller channels branching out to the individual orifice locations.

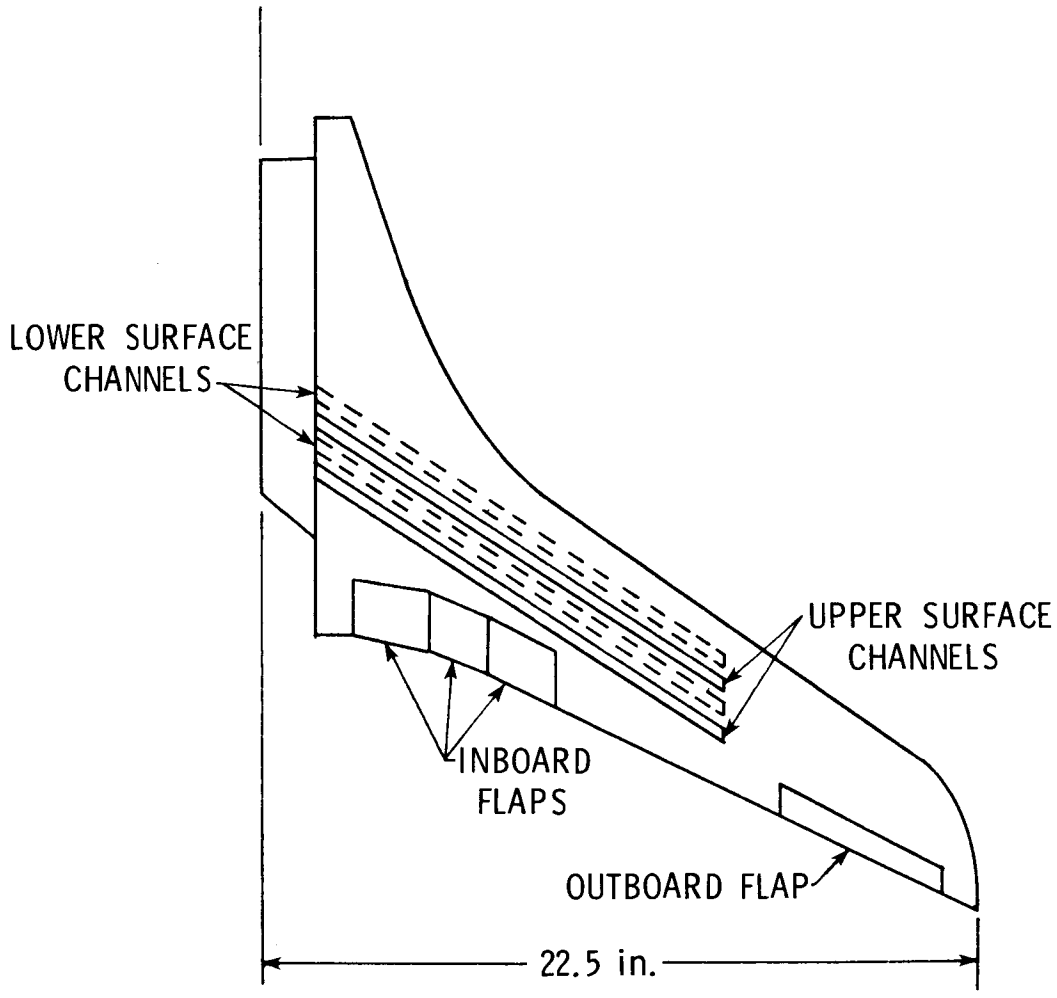

Figure 2

SPAR MODEL OF ATT WING

The ATT wing was modeled in SPAR using plate elements as shown in figure 3. This element type has been shown to give accurate predictions of deflections for metal wings with small internal or surface channels (see refs. 2, 8, and 9). In addition, using plate elements rather than beam elements permits the calculation of wing camber changes due to aerodynamic loading. The close chordwise spacing of the nodes in the mid-chord region was required in order to define the instrumentation channels. The number of nodes in the spanwise direction was determined from a convergence study in which the number of nodes was increased until there was no change in the calculated deflections. The control surfaces were modeled using unconnected coincident points at the sides of the segments to allow them to deform independently of the other segments and the main wing. The flap attachment tab was represented by short, thin elements. A cantilever constraint was applied at the outboard edge of the first row of elements, corresponding to the side of the fuselage.

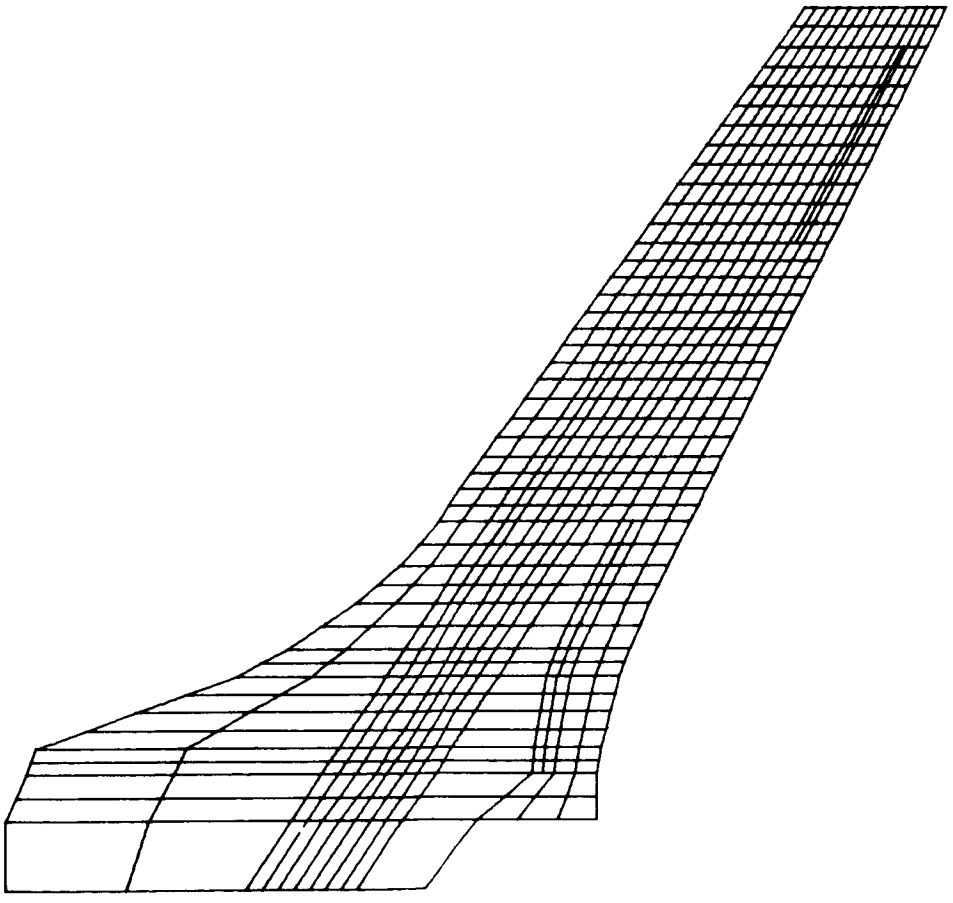

Figure 3

CROSS SECTION OF ATT WING AS MODELED IN SPAR

A representative cross section of the finite-element model, along with the actual cross section of the wing, is illustrated in figure 4. As can be seen, the four main channels remove a substantial amount of metal in an area that is important to the bending stiffness of the wing. The plate thicknesses were determined by averaging the thicknesses at the four nodes defining the plate. The thickness at a node at the leading edge was increased from zero to one-third the thickness at the next streamwise node to give a more accurate representation of that region of the wing. The vertical location of a node was midway between the upper and lower surface of the wing (or the bottom of a channel) at that location. The flap attachment tab was not offset vertically but was set to the actual tab thickness. No attempt was made to model the small channels leading from the main channels to the orifice locations.

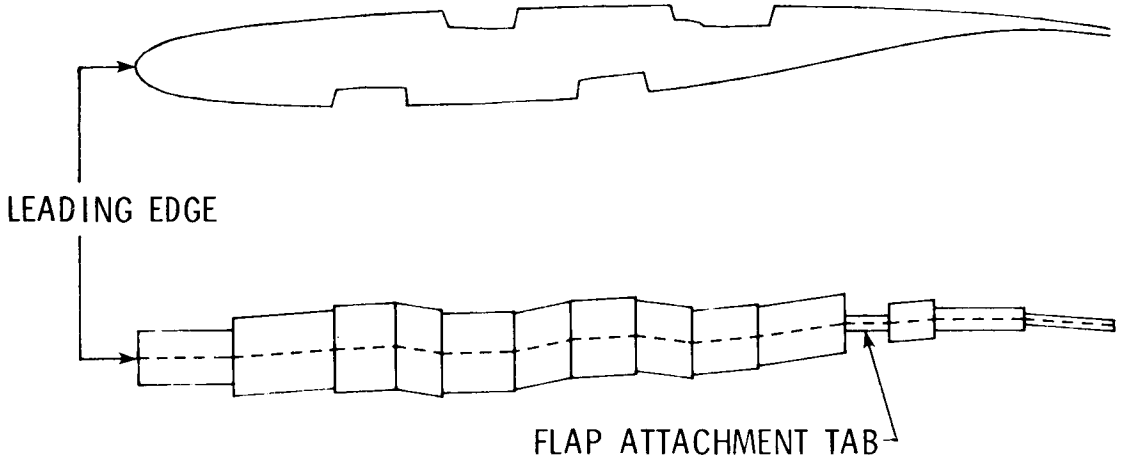

Figure 4

ATT MID-SEMISPAN WING PRESSURE DISTRIBUTIONS CALCULATED USING WIBCO

In the wind tunnel tests of the ATT model (ref. 6), several runs were made at a Mach number of 0.90 but at different total pressures in an attempt to examine Reynolds number effects. The wing pressure distributions from these runs indicated that the anticipated rearward shock movement with increasing Reynolds number did not occur; instead, the shock moved forward and weakened. This is what would happen if the increase in dynamic pressure (resulting from the increase in total pressure to obtain the higher Reynolds number) caused a significant increase in the aeroelastic washout of the wing. Two of the test conditions were run in TAPS to see if these changes could be accurately predicted.

The tunnel Mach number of 0.90, Reynolds numbers (based on mean aerodynamic chord) of 1.58 and 4.87 million, and dynamic pressures of 536 and 1613 psf were used as input for TAPS. When comparing pressure distributions calculated with transonic potential flow codes it is often necessary to analyze the configuration at an angle of attack that differs from the experimental angle to improve the correlation between theory and experiment. Since the primary interest in this example was predicting pressure changes due to aeroelastic and Reynolds number effects, the angle of attack was increased by 1.14 degrees in the calculations to give better agreement with the experimental upper surface pressures at the lower dynamic pressure condition. This increment was then maintained in the calculations for the higher dynamic pressure case. The change in angle of attack is larger than normally required, but this would be expected since previous correlations did not account for the reduction in wing loading caused by model deformations.

The axisymmetric fuselage option in WIBCO was used for these calculations. The computational wing plane was originally located to match the low wing of the wind tunnel model, but this resulted in instabilities in the calulations, so the wing plane was shifted toward mid-fuselage. Boundary layer transition locations were set to correspond to the transition strip locations given in reference 7.

The calculated pressure distributions at $\eta = 0.54$ for the two cases are shown in figure 5 along with the corresponding experimental results. The changes in pressure levels between the two cases caused by changing Reynolds number and dynamic pressure were predicted reasonably accurately on the upper surface ahead of the shock, but the shock locations and the pressure changes aft of the shock did not correlate well at all. This is probably related to the non-conservative finite-difference scheme used in WIBCO, which tends to calculate shock locations that are too far forward. The lower surface pressure increments were predicted fairly well.

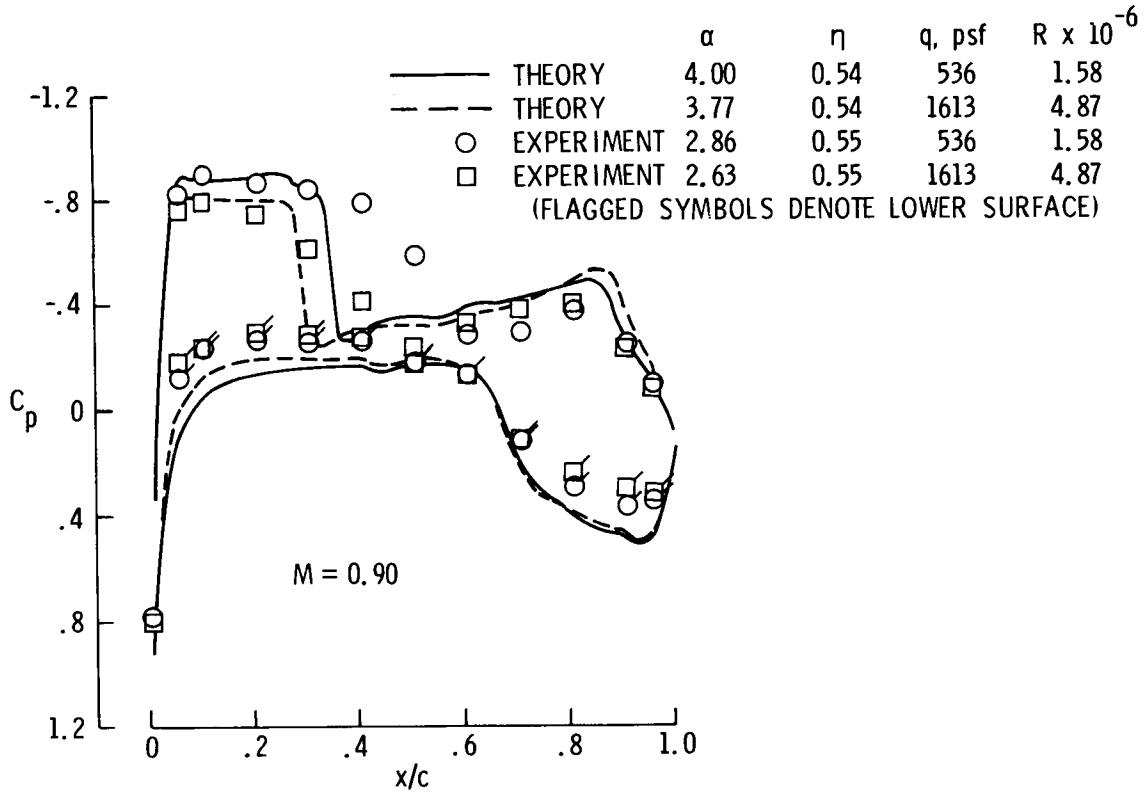
α η q, psf R x 10^-6
THEORY 4.00 0.54 536 1.58
THEORY 3.77 0.54 1613 4.87
EXPERIMENT 2.86 0.55 536 1.58
EXPERIMENT 2.63 0.55 1613 4.87
(FLAGGED SYMBOLS DENOTE LOWER SURFACE)
-1.2
-.8
-.4
C_p 0
.4
.8
1.2
M = 0.90
0
.2
.4
.6
.8
1.0
x/c

Figure 5

ATT OUTBOARD WING PRESSURE DISTRIBUTIONS CALCULATED USING WIBCO

Figure 6 shows the theoretical and experimental pressure distributions for the ATT at about η = 0.72. The pressure changes ahead of the shock are again predicted fairly well, but the shock near mid-chord is calculated to be much too far forward for the lower dynamic pressure case, resulting in poor correlation between theoretical and measured pressure increments over the last half of the airfoil. The good prediction of the upper surface pressure distribution for the higher pressure case with its weaker, more forward shock can be attributed to the aeroelastic twist reducing the angle of attack and thus presenting an easier case for the aerodynamic code to solve. The calculated aeroelastic twist increments at this wing station were about -0.9° and -2.5° for the low and high dynamic pressure cases, respectively.

Even with the poor correlation between theory and experiment in some areas, it is obvious that the large changes in the experimental pressure distribution were at least qualitatively predicted using TAPS, emphasizing the importance of including aeroelastic effects in transonic calculations. The correlation should improve as more accurate aerodynamic codes are incorporated into TAPS.

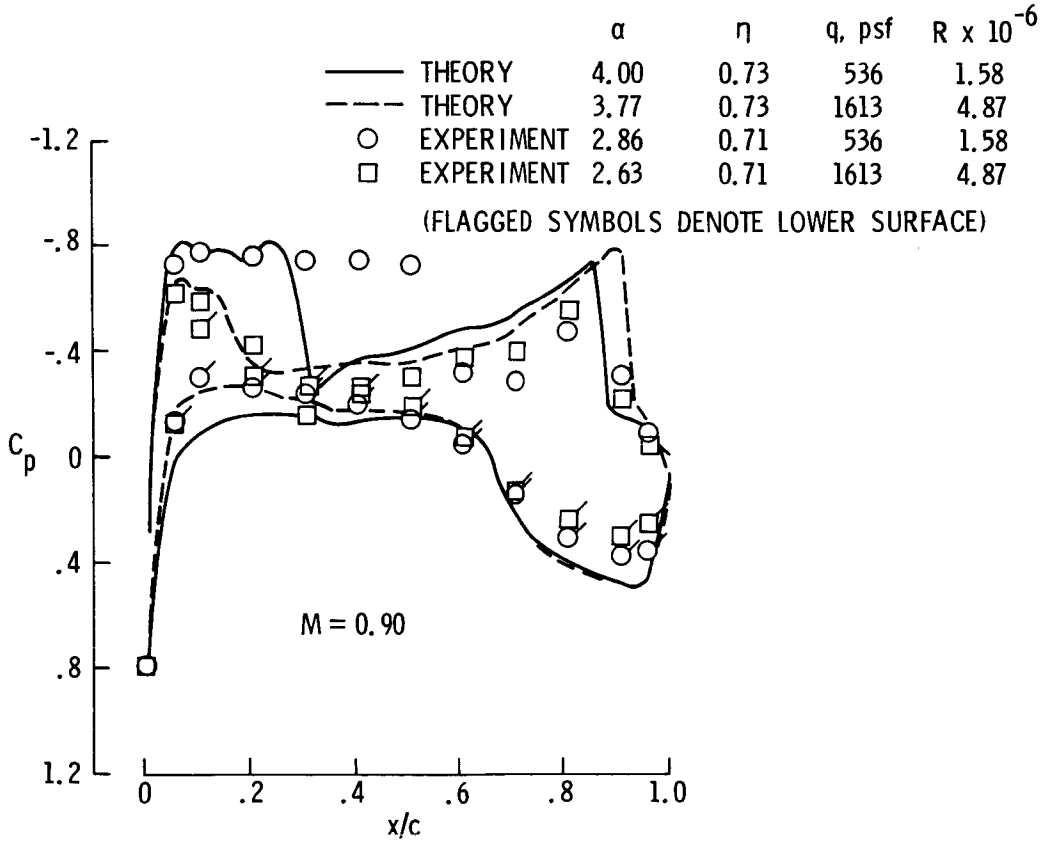

Figure 6

CALCULATED EFFECTS OF INDEPENDENT VARIATION OF REYNOLDS NUMBER AND DYNAMIC PRESSURE

The TAPS analysis method can be used to predict what changes would have been seen in the ATT pressure distributions if the Reynolds number could have been increased without changing the dynamic pressure. This is shown in figure 7 along with the effects of changing dynamic pressure while maintaining a constant Reynolds number. As can be seen, there is not much of an effect on the pressure distribution caused by increasing just Reynolds number. The thinner boundary layer at the higher Reynolds number does not reduce the effective trailing edge camber as much, causing the second shock to be slightly farther aft than in the lower Reynolds number case. Changing the dynamic pressure had a much greater effect at these conditions for this configuation. The shock near mid-chord moved forward and weakened considerably while the second shock moved slightly aft in the higher dynamic pressure case. The lower surface pressure coefficients became more negative, as expected, from the aeroelastic washout.

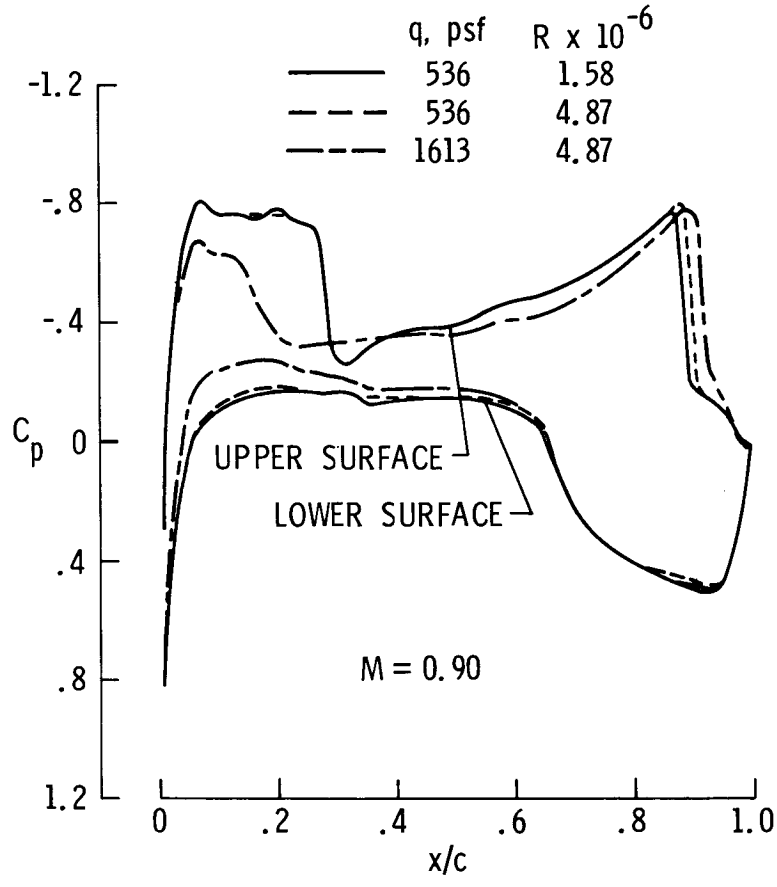

Figure 7

ATT MID-SEMISPAN PRESSURE DISTRIBUTIONS CALCULATED USING TAWFIVE

Recently, the fully conservative full-potential TAWFIVE code was substituted for WIBCO as the aerodynamic module in TAPS. The two test conditions for the ATT configuration were run in this new version of TAPS to see if the predicted pressure distributions could be improved, especially with regard to shock location. The TAWFIVE code was somewhat more difficult to run than WIBCO in that both the inviscid and boundary layer components showed some instabilities initially. The aerodynamic model had to be changed to a mid-wing configuration and the sweep of the leading-edge glove had to be reduced near the side of the fuselage in order to eliminate these instabilities. The input flow conditions were the same as those used for the WIBCO runs, including the angle-of-attack increment of 1.14° added to the experimental angles.

Figure 8 shows the resulting pressure distributions for the ATT cases at about $\eta = 0.55$. Overall, the correlation is very good. The shock location is predicted very well for the low dynamic pressure case, but is slightly too far aft in the high dynamic pressure calculations. The upper surface pressure coefficient level for the latter case is also slightly too negative, indicating that the angle of attack for this wing station is too high. The predicted lower surface pressure coefficients are too positive, but are in closer agreement with the data than were the WIBCO predictions (see figure 5). In general, the pressure increments and shock movement calculated using TAPS with TAWFIVE correlated reasonably well with the experimental results at this wing station.

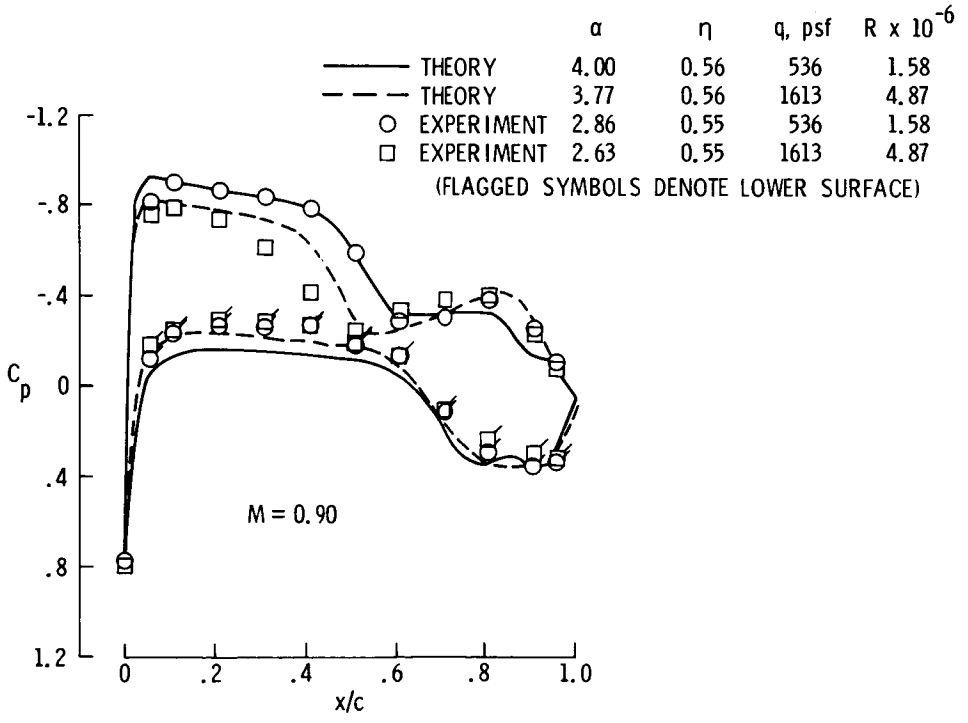

ATT OUTBOARD PRESSURE DISTRIBUTIONS CALCULATED USING TAWFIVE

Figure 9 shows the calculated and experimental pressure distributions for the ATT configuration at about $\eta = 0.72$. As at the mid-semispan station, the correlation between theoretical and experimental shock location and pressure levels is good for the low dynamic pressure case. For the high dynamic pressure condition, the upper surface pressure coefficients ahead of the shock are too negative, again indicating that the local angle of attack is too high. This would also cause the calculated shock location to be too far aft, since the supercritical airfoil section used is very sensitive to angle of attack. It appears that the theoretical model of the wing may be too stiff, possibly because it does not account for the effects of the small channels to the pressure orifice locations. It is interesting to note, however, that the twist increments calculated using TAWFIVE were within two percent of the values predicted using WIBCO, and the pressures calculated by WIBCO showed good agreement with the experimental pressures for the high dynamic pressure case. It is also possible that the pressures near the wing tip, which have a large effect on the wing deflections, may not be calculated correctly, but no data were available for comparison outboard of $\eta = 0.71$. A third possible source of the discrepancy is that the theory-to-experiment angle increment of 1.14° determined using WIBCO is larger than that required for TAWFIVE. The pressure increments due to changing dynamic pressure and Reynolds number were predicted qualitatively on the lower surface, with the predicted increment being slightly too large.

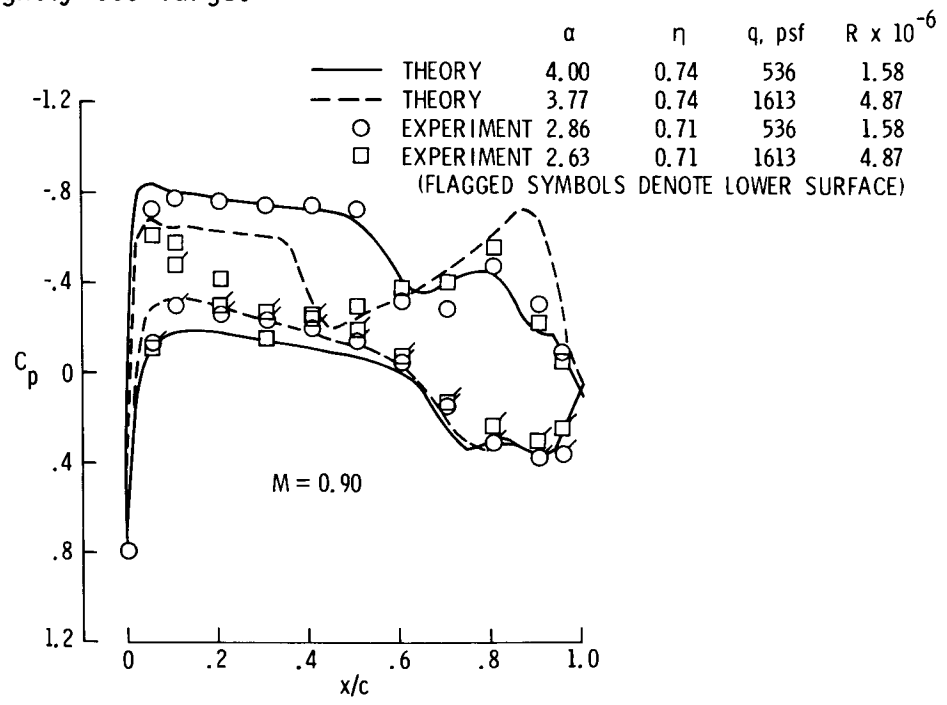

Figure 9

TF-8A GEOMETRY AND SPAR MODEL DESCRIPTION

The second configuration used as a test case in TAPS was the TF-8A model described in reference 10. A top view of the SPAR model of the wing is shown in figure 10. The wing had a span of 32.34 in., a quarter-chord sweep of 42.24°, an aspect ratio of 6.8, and a taper ratio of 0.36. The NASA supercritical airfoil sections varied in maximum thickness-to-chord ratio from 0.114 near the fuselage to 0.071 near the tip. This configuration also had a highly swept leading-edge glove that extended to approximately $\eta = 0.35$.

The TF-8A wing was fabricated from solid aluminum with surface channels for the pressure instrumentation. No attempt was made to include these channels in the SPAR model since their geometry was not defined in the available references. A 12 x 50 node grid was generated, extending from the wing symmetry plane to the tip. Plate element thicknesses and the vertical location of the nodes were determined as described for the ATT model. A cantilever constraint condition was enforced at the wing symmetry plane.

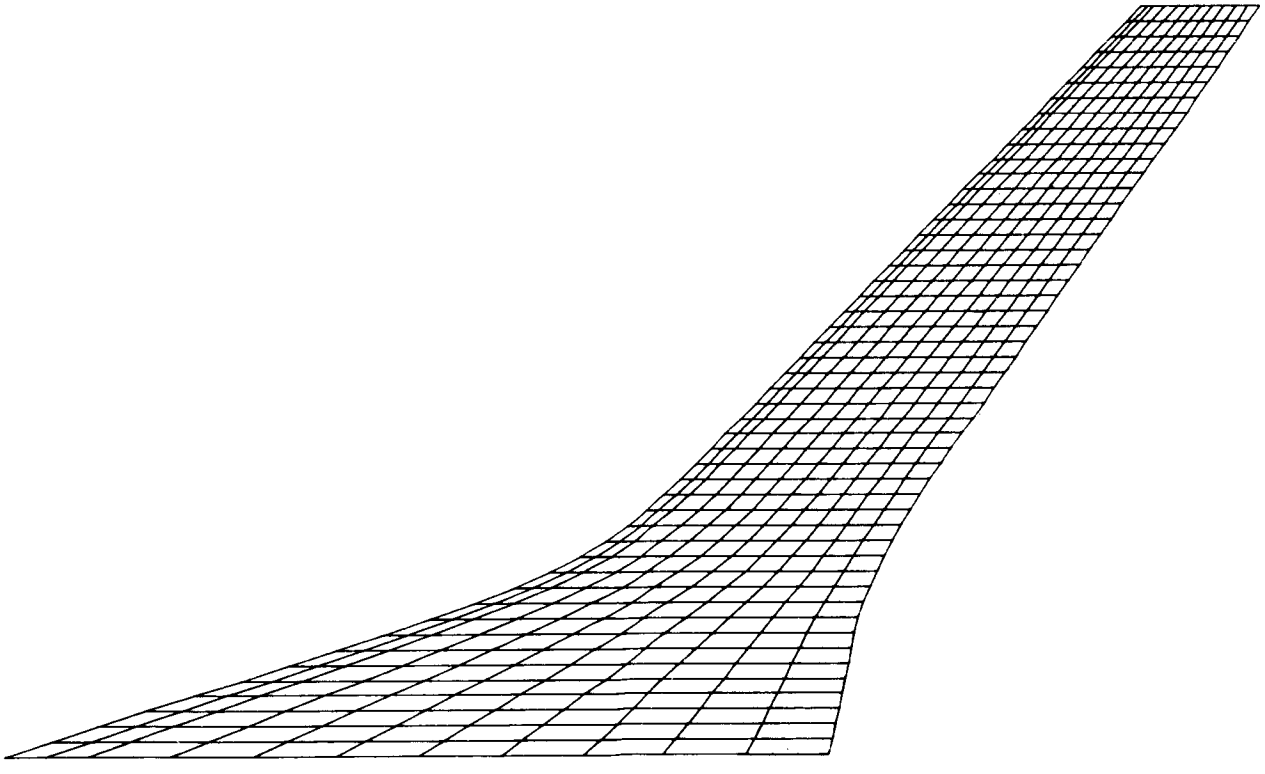

Figure 10

TF-8A MID-SEMISPAN WING PRESSURE DISTRIBUTIONS CALCULATED USING WIBCO

Two test conditions for the TF-8A were run in TAPS using the tunnel Mach number of 0.95, dynamic pressures of 425 and 850 psf, and Reynolds numbers (based on the mean aerodynamic chord) of about 1.0 and 2.0 million. The experimental angle of attack was increased from 4.0° to 4.6° to try to improve the theory-experiment correlation at the lower dynamic pressure condition. A mid-wing location on an axisymmetric fuselage was used in WIBCO. The theoretical boundary layer transition locations were matched to the transition strip locations on the wind tunnel model.

The resulting pressure distributions are presented along with the experimental results in figures 11 and 12. As can be seen in figure 11, the correlation between theory (with the angle-of-attack adjustment) and experiment is good at about the mid-semispan station. The shock which occurs experimentally around $x/c = 0.3$ on the upper surface is not predicted by the theory, which instead calculates an isentropic compression of about the same pressure increase in that region. Also, the predicted lower surface pressure coefficients are somewhat more positive than the experimental values. Except for a small region near the leading edge and the area just aft of the shock, the increments in the experimental pressures caused by changing Reynolds number and dynamic pressure, though small, were predicted reasonably well.

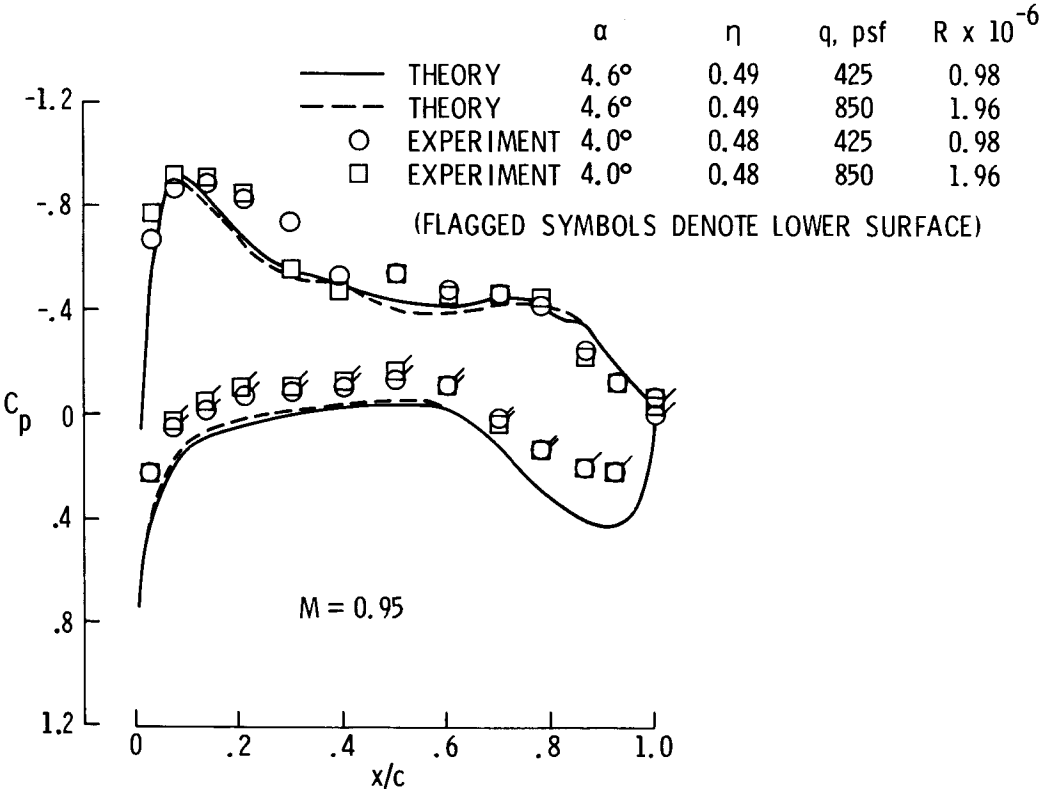

Figure 11

TF-8A OUTBOARD WING PRESSURE DISTRIBUTIONS CALCULATED USING WIBCO

The correlation between theoretical and experimental pressure distributions for the TF-8A deteriorates at η = 0.80 (figure 12). The predicted shock location is much too far forward and is followed by a re-expansion of the flow and a second shock that is not present in the data. Pressure coefficients on the upper surface near the leading edge were calculated to be more negative than the experimental values and lower surface pressure levels did not correlate well anywhere. The poor correlation in shock location and leading-edge pressures can probably be attributed to the non-conservative differencing and the small-disturbance approximation, respectively, used in WIBCO. It is likely that the correlation for this case could also be improved by using the TAWFIVE version of TAPS. It should be noted that the changes in pressure levels at this wing station resulting from the change in Reynolds number and dynamic pressure were predicted fairly accurately except near the shock. This would indicate that the integrated effect of the loads on the wing resulted in approximately the correct change in wing shape.

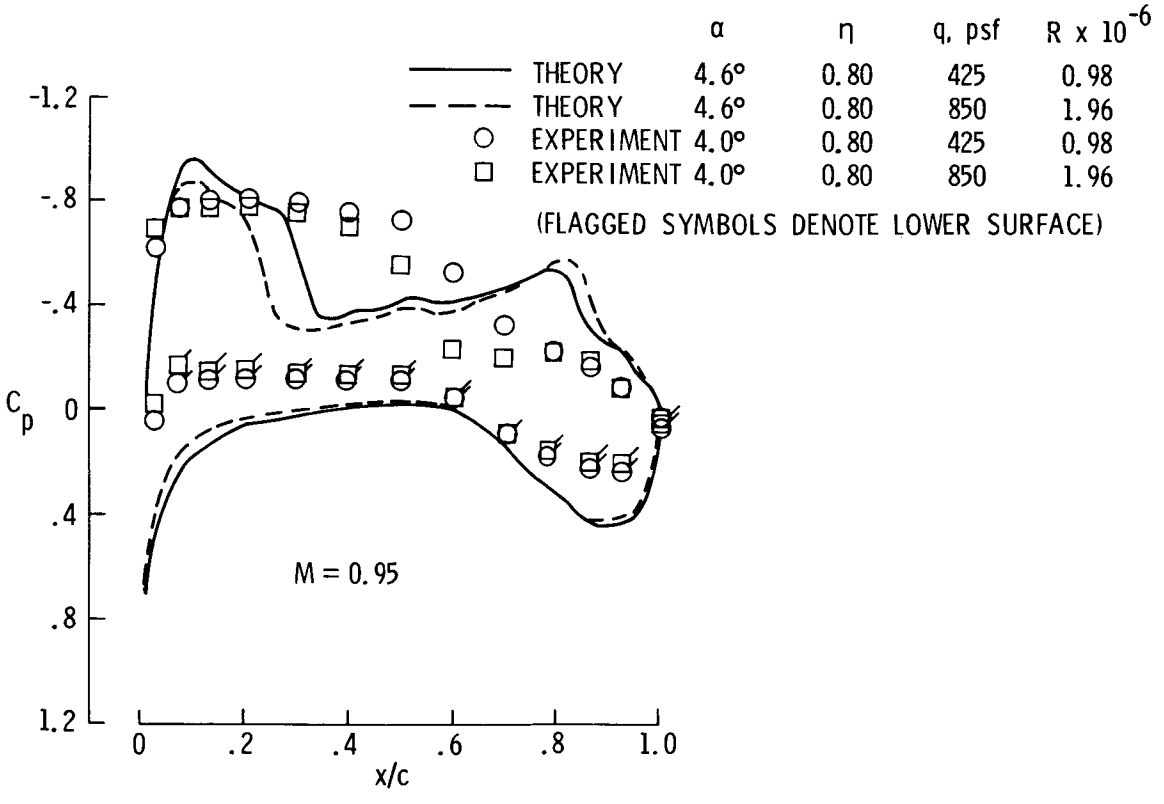

Figure 12

STATIC AEROELASTIC TWIST DISTRIBUTIONS FOR THE TF-8A MODEL

The spanwise distributions of aeroelastic twist corresponding to the pressure distributions shown in figures 11 and 12 are given in figure 13. The experimental values were obtained during the wind tunnel test of the model using stereophotogrammetry as described in reference 10. The calculated values agree very well with the experimental data for both the low and high dynamic pressure cases; the twist increment at the tip for the high dynamic pressure case is overpredicted by about 0.2° which according to reference 9 is within the accuracy of the data. While the agreement is good, it should be noted that this is partly due to the offsetting effect of some errors. The pressure distributions shown in figures 11 and 12 indicate that the calculated lift is greater and the pitching moment more negative than the experimental values, which would result in the predicted twist being too large. However, since the wing channels were not modeled, the theoretical model is stiffer than the actual wing, thereby compensating to some extent for the higher calculated loads.

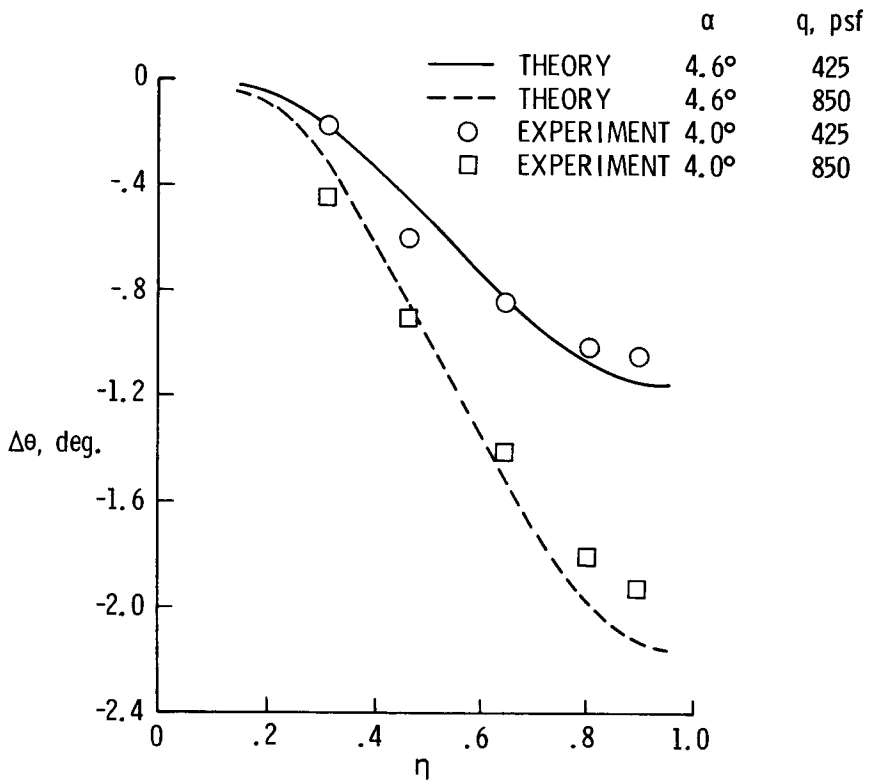

Figure 13

CONCLUSIONS

A simple method of including aeroelastic effects in 3D transonic calculations has been developed. Known as the Transonic Aeroelastic Program System, or TAPS, the method couples a transonic computer code with a finite element structural analysis program in an iterative fashion. The calculations for this study were made using the SPAR structural analysis code with either the small-disturbance WIBCO code or the full-potential TAWFIVE code as the aerodynamic module. Both aerodynamic codes used interactive boundary layer calculations to model viscous effects. Calculated results from TAPS were compared with data for two test cases. The following conclusions were drawn from this study (see figure 14):

1. TAPS gave fairly good predictions of pressure increments due to changes in Reynolds number and dynamic pressure, except near shocks.

2. The TAWFIVE version of TAPS generally gave more accurate predictions of the pressure distributions (especially shock locations) than did the WIBCO version for the configuration and conditions used in this study. WIBCO did give better correlation at the outboard station for the high dynamic pressure case.

3. Wing deflections calculated using TAPS correlated well with deflections optically measured in a wind tunnel.

- TAPS PROVIDES A SIMPLE METHOD OF INCLUDING AEROELASTIC EFFECTS IN TRANSONIC CALCULATIONS.
- TAPS GAVE FAIRLY GOOD PREDICTIONS OF PRESSURE INCREMENTS DUE TO CHANGES IN REYNOLDS NUMBER AND DYNAMIC PRESSURE, EXCEPT NEAR SHOCKS.
- TAPS/TAWFIVE GENERALLY GAVE MORE ACCURATE PREDICTIONS OF PRESSURE DISTRIBUTIONS (ESPECIALLY SHOCK LOCATIONS) THAN TAPS/WIBCO.
- WING DEFLECTIONS CALCULATED USING TAPS CORRELATED WELL WITH DEFLECTIONS OPTICALLY MEASURED IN A WIND TUNNEL.

Figure 14

SYMBOLS

C_p	pressure coefficient
M	free-stream Mach number
q	dynamic perssure, psf
R	Reynolds number based on mean aerodynamic chord
x/c	chordwise station
α	angle of attack, degrees
$\Delta\theta$	static aeroelastic twist increment, degrees
η	semispan station

REFERENCES

1. Fuller, Dennis E.: Guide for Users of the National Transonic Facility. NASA TM-83124, July 1981.

2. Campbell, Richard L.: A Computational Method for Predicting the Effects of Varying Reynolds Number and Dynamic Pressure on Flexible Wings at Transonic Speeds. Masters Thesis, George Washington University, February 1984.

3. Boppe, Charles W.: Transonic Flow Field Analysis for Wing-Fuselage Configurations. NASA CR-3243, 1980.

4. Melson, N. Duane; and Streett, Craig L.: TAWFIVE - A Users' Guide. NASA TM-84619, September 1983.

5. Whetstone, W. D.: SPAR Structural Analysis System - Reference Manual, Vol. I, NASA CR-145098-1, February 1977.

6. Struzynski, N. A.: Transonic Wind Tunnel Tests of a Model of the Advanced Technology Transport. Calspan No. T18-073, November 1973.

7. Mann, Michael J.; and Langhans, Richard A.: Transonic Aerodynamic Characteristics of a Supercritical-Wing Transport Model With Trailing-Edge Controls. NASA TM X-3431, October 1977.

8. Mehrotra, S. C.; and Gloss, B. B.: Computation of Wind Tunnel Model Deflections. AIAA-81-0482-CP, Atlanta, Georgia, April 1981.

9. Mehrotra, S. C.; and Robinson, J. C.: Structural Modeling of High Reynolds Number Wind Tunnel Models. AIAA-82-0602-CP, Williamsburg, Virginia, March 1982.

10. Brooks, Joseph D.; and Beamish, Jerry K.: Measurement of Model Aeroelastic Deformations in the Wind Tunnel at Transonic Speeds Using Stereophotogrammetry. NASA TP-1010, October 1977.